

# APPLICATION OF LINEAR X-RAY ANALYSIS USING ABSORPTION COEFFICIENTS FOR DIRECT DETERMINATION OF IN SITU CORE SATURATION FOR PC MEASUREMENT

E. A. Spinler and D. R. Maloney  
Phillips Petroleum Co.

## ABSTRACT

Measurement of the in situ distribution of fluid saturation in a rock sample is a prerequisite for determination of capillary pressure ( $P_c$ ) curves by the Direct Measurement of Saturation (DMS). A common method for measurement of fluid saturation in rock is linear x-ray scanning. The use of linear x-ray for  $P_c$  measurement by DMS has not previously been reported. Lambert's equation provides a means to accurately quantify fluid saturation using an x-ray scanning technique. The equation relates the intensity of an x-ray beam that emerges from a saturated rock to the incident beam intensity, and the absorption coefficients and thickness of rock matrix and fluids that occupy the pore space.

To demonstrate the application, imbibition  $P_c$  curves were obtained by linear x-ray measurements for four Kansas outcrop chalk plugs. The wettability of three of these plugs had been altered to illustrate the different  $P_c$  curves that could be obtained. The procedures used cells containing the saturating fluids, air, octadecane, and brine to obtain accurate determination of the absorption coefficients before saturating the rock samples. Subsequently, the plugs were saturated and spun by centrifuge with a free water level to obtain the positive and negative portions of the imbibition  $P_c$  curves. Accurate measurement of the free water level can be obtained from images obtained by magnetic resonance (MRI) or by x-ray scanning techniques. A reference rock sample provided control over experimental variations.

## INTRODUCTION

It has only been in recent years that direct determination of capillary pressure ( $P_c$ ) by DMS has become a recognized technique with significant technical advantages over all other  $P_c$  techniques.<sup>1,2,3,4</sup> Most  $P_c$  curves continue to be determined by mercury intrusion, porous plate/membrane or conventional centrifuge methods.

Techniques like mercury intrusion,<sup>5,6</sup> although rapid and popular, provide questionable results due to the use of mercury in a vacuum to mimic water/oil behavior. The methodology limits the technique to primary drainage and positive imbibition capillary pressures. A mercury derived  $P_c$  curve is at best constrained to only highly water-wet behavior at positive  $P_c$ . Porous plate/membrane methods<sup>7,8,9,10,11</sup> can generate all the hysteresis  $P_c$  curves, but they can be slow to obtain apparent equilibrium saturation. Each measurement point must be determined individually and the technique is limited by membrane/porous plate technology. Some efforts have tried to improve the speed,<sup>12</sup> but the technique is still tedious. The centrifuge method is normally only used to determine drainage or negative imbibition curves. Others<sup>13,14,15,16</sup> have developed modified and/or more complex techniques to obtain positive imbibition  $P_c$  curves in the centrifuge. Use of the centrifuge is generally more rapid than porous plate/membrane methods, but it also measures only a single point at a time and can be

time consuming to obtain equilibrium data. Another major limitation of these types of centrifuge methods is that they can only provide an indirect, or assumed/calculated, measure of saturation at the inlet face of a rock plug based on the amount of fluid that has entered into or been expelled from the rock. Numerous methods over the past 50 years<sup>17</sup> have been proposed for approximating the inlet saturation from centrifuge effluent volumes, but in every case, the model can influence the resultant capillary pressure curves. Other methods using in-situ images from flow experiments<sup>18</sup> have yet to demonstrate that they can accurately determine spontaneous imbibition Pc curves and appear to also be model dependent.

In contrast, DMS for Pc is a rapid measurement with the possibility of over 100 measurements made along a Pc curve simultaneously. It can measure all of the hysteresis Pc curves and achieve apparent equilibrium for a complete curve in the time required for a single measurement by typical centrifuge or porous membrane/plate techniques. It can avoid all of the errors associated with the non-uniform centrifuge pressure field. It is also applicable to heterogeneous rock, non-uniform wettability and low to high permeability rock.<sup>19</sup> Since it uses a direct measurement of saturation, no model is required for interpretation and the resultant data, if obtained properly, can provide the true equilibrium Pc curve for the system that is measured.

One limiting factor to the broad application of DMS for Pc in the industry may be the availability of imaging technology to accurately quantify saturation. Most publications to-date have used magnetic resonance imaging as the choice for measurement of internal saturations for Pc by DMS. Some other imaging techniques have been demonstrated as quite capable, such as gamma adsorption.<sup>4</sup> One of the more common tools to look at internal fluid saturation is through the use of linear x-ray imaging, which is addressed in this paper.

This paper provides a practical application of x-ray theory to obtain complete Pc curves using DMS. Its purpose is to describe the methodology using linear x-ray imaging in sufficient detail to facilitate employment of the DMS technology by others in the industry.

## **EQUIPMENT, MATERIALS, METHODS**

Four plugs of Kansas outcrop chalk were the porous medium used in this experimental study. The physical properties for the plugs as determined by Boyle's law and air permeability are listed in Table 1. These values are typical for most chalk reservoirs in that permeability is low and porosity is high. Since the rock was outcrop material and originally had not been exposed to crude oil, it was believed to be initially highly water-wet. Its wettability was altered by stearic acid (octadecanoic acid) that was dissolved in n-decane at varying concentrations and aged at elevated temperature and various lengths of time to render it less water-wet. Tang and Firoozabadi<sup>20</sup> have published the details of the aging and preparation procedure used for these plugs.

The plugs were received clean and dry with three of them already having an altered wettability. The work requested on these plugs was to obtain the positive and negative portions of the capillary imbibition curves using the DMS method. The initial state of the plugs for the measurement of Pc was requested to be 100% oil saturated.

Kansas outcrop chalk often contains high concentrations of iron as pyrite and other forms. Iron-containing minerals diminish the quality of magnetic resonance imaging (MRI) measurements. Consequently, the use of MRI was not a viable means of measuring internal saturations for Pc determination. On the contrary, x-ray absorption techniques are applicable even when the porous media contains pyrite. Linear x-ray techniques are more

commonly used in the industry to obtain internal fluid saturations. For these reasons, it was chosen as the means to obtain internal core saturation information in this study.

The brine used in this experiment contained 5,000 ppm potassium chloride with 25,000 ppm potassium iodine (KI). Octadecane was the oil phase. The high concentration of KI in the brine was chosen to enhance the x-ray absorption contrast between solid octadecane and the brine. Octadecane has a melting point at 27°C and is a solid at room temperature (about 22°C) when x-ray measurements were made.

Linear x-ray measurements were obtained using a scanner previously described by Maloney, et al.<sup>21</sup> An image intensifier was used to gain 2-D images of the rock. The image intensifier provides 'shadow' images from x-rays that pass through the entire sample rather than through a slice. Changes in the brightness of x-ray images (gray scale intensities) are related to changes in fluid saturations.

The plugs were marked so that the same portion of the plug can always be imaged. They were then sleeved in heat-shrink tubing with the ends open. This was done to confine all movement of the brine and octadecane during the determination of the imbibition Pc curve to co-current imbibition displacement.

The wettability distribution in each plug was obtained by counter-current spontaneous imbibition in a heated oven. The plugs were cooled under brine and x-ray measurements were taken after each imbibition step at room temperature to obtain the saturation profiles. Weight measurement was used to monitor the imbibitions and to determine the contraction of octadecane from solidification.

## MEASUREMENTS AND CALCULATIONS

### *Initial Calibration*

Lambert's equation<sup>22</sup> provides a basis for understanding the adsorption of x-rays. A corollary<sup>23</sup> to that equation simplifies its application. If the incident intensity remains constant, and spacing between the x-ray source, the sample and the detector remains constant, the corollary is:

$$I = I_0 \exp[-(\mu_A t_A + \mu_B t_B + \mu_C t_C + \dots)] \quad (1)$$

$I_0$  and  $I$  are emergent beam intensities.  $I_0$  is the emergent intensity at a reference condition, while  $I$  is the emergent intensity after a change in the absorption characteristics or change in thickness of absorbers in the beam path. The thickness variable,  $t$ , represents the change in thickness of an absorber from the reference condition. The variable,  $\mu$ , represents the absorption coefficient of one of the variable absorbers in the beam path. The absorption coefficient is a constant that must be measured independently. Subscripts, A, B, C, ... are to distinguish between different absorbers.  $I_0$  can be measured to account for all other materials, such as the rock matrix and coreholder in the beam path that are expected to be constant in thickness.

The method employed to apply the corollary to Lambert's equation for this experimental work required that we determine the value for five unknowns,  $I_0$ ,  $\mu_W$  and  $t_W$  for the brine and  $\mu_O$  and  $t_O$  for the solid octadecane. Reference images for  $I_0$  were made with two empty plastic cells in front of each plug while dry to obtain the combined x-ray absorption of the plug rock matrix, the confining sleeve and the cells. This configuration (Figure 1) with plastic cells became part of the system for all subsequent images as will be explained. They

could have easily been treated as another absorber, but this would require determination of values for two additional unknowns and an added x-ray image per plug.

The plugs were cylindrical in shape. This created geometrical artifacts for the x-ray image as well as other geometrical artifacts that are introduced by the centrifuge.<sup>24</sup> Two adjustments were made to minimize these artifacts. First, the analysis of the image was limited to a 4 millimeter wide slice (approximately 26 pixels) through the center of the plug in the same plane as the centrifuge axis (illustrated in Figure 2). This essentially reduced the circular shape of the induced centrifuge force field relative to the plug shape to insignificance and any other correction for centrifuge effects was unnecessary. Gravity artifacts (Figure 3) were also evaluated and found for these cases to be insignificant with respect to the reported results. The x-ray image was 9-11 millimeters wide as controlled by the shutter settings on the image intensifier. By limiting the analyzed data to only a 4 mm slice in the center of the image, it was also possible to eliminate smearing of the analyzed portion of the image from edge effects. These edge effects can be caused by x-ray reflections, etc. that distort the x-ray image (Figure 4). The ideal x-ray response for a uniform porosity rock would show increasing brightness in the image from moving off center because the thickness of the cylindrical plug diminishes. So a second adjustment was made to account for the varying thickness of the rock plug by averaging the ideal thickness of the plug over the 4 mm width.

The absorption coefficients of the brine and solid octadecane were obtained prior to saturating the core plugs. This was accomplished by obtaining a series of x-ray images conducted by scanning dry plug samples through plastic cells emptied and filled with various thicknesses of brine, and solid octadecane. Ideally, it was possible to use a single cell of a known and precise thickness filled with the brine and subsequently with solid octadecane to obtain the absorption coefficients. However, although the cells were made with care, our more prudent approach was to use several cells providing various thicknesses of the fluid and solid to obtain the absorption coefficients. Small errors in the thickness of each absorbent and in the statistical nature of x-ray images would then tend to average out. For these plugs 6 different thickness of oil and water were used requiring 6 x-ray images per plug. Each image consisted of 100 image acquisitions that were averaged to form a single image. The time to obtain such an image took 10 seconds. Images were made with the following thicknesses, 0.5 cm brine, 1 cm brine, 1.5 cm of brine, 0.5 cm of solid octadecane, 0.5 cm of brine with 0.5 cm of solid octadecane and 1 cm of brine with 0.5 cm of octadecane. The x-ray intensity across the 4 mm width was averaged along the length of each plug for each image. A non-linear least squares routine was then used to obtain the best values for the absorption coefficients from the averages for all of the measurements on all of the plugs simultaneously. The obtained absorption coefficient values were 0.74305 and 0.1276 for the brine,  $\mu_w$ , and the solid octadecane,  $\mu_o$ , respectively.

The completion of imaging cycle to obtain a set of Pc curves by the DMS method is a relatively rapid process, but can be delayed from weeks to months to complete depending upon competing priorities for x-ray equipment. In our labs, a particular x-ray apparatus may work on as many as 3 experiments at a time with the x-ray source and intensifier being moved extensively between x-ray images. As an added precaution against fluctuations in x-ray images from small positioning errors of the plugs relative to the x-ray source and the intensifier, a dry chalk plug was selected to be a reference plug. It was sleeved and the ends sealed. Since it would not change significantly with time, it was always imaged at each step in the image cycle to confirm positioning and, if necessary, to provide a means for adjustment of small image intensity variations.

### ***Porosity determination***

Knowing these coefficients, it was possible to determine the local porosity distribution in the plugs along the 4 mm width of the x-ray image. The plug was vacuum and pressure saturated (2500 psi for 16 plus hours) with the brine. This enabled a confirmation of the bulk plug porosity, previously measured. With only one fluid in the pore spaces of the plug, solving for the average brine thickness at each pixel height position using Lambert's corollary and subsequently a local porosity was straightforward. These porosity curves are provided with the  $P_c$  curves that are described below. The thickness of the water obtained in this step provided the additional equation to solve locally for the 2 remaining unknowns,  $t_o$  and  $t_w$ , when both brine and solid octadecane saturate the plug.

$$\text{Thickness from porosity} = t_\phi = t_o + t_w \quad (2)$$

### ***Pc determination***

To obtain an imbibition  $P_c$  curve starting from a 0% water saturation state in the plugs, they were flushed with multiple pore volumes of deionized water to remove the salts and then dried. To saturate the plugs with octadecane required a different procedure than saturating with brine because it is a solid at room temperature. The dried plugs were packed in sand and centrifuged under octadecane at 40° C using an angle head for 24 hours with two 180° rotations and one inversion. Prior to final removal from the centrifuge, the plugs were chilled to 15° C while centrifuging to solidify the octadecane. Since it is difficult to remove all of the octadecane from the outside of the plugs, gravimetric confirmation of the saturation state of the plug was not accurate. Using Lambert's corollary, the thickness of the octadecane was calculated in the same manner as the brine thickness and compared to the brine thickness. The comparison showed the plugs were not fully saturated with octadecane with the saturation state ranging from 86 to 89%. The centrifuge process was repeated and the plugs were re-imaged. In this case the calculated saturations for the plug improved to 95-97%. For practical purposes this was considered adequate for starting the DMS method for  $P_c$ . The air remaining in the plugs was isolated and the first step of the DMS procedure would be to centrifuge the plugs for 2 weeks. Additional centrifugation and invasion of brine would be expected to displace all of the remaining air.

The DMS method for  $P_c$  is described in detail by Spinler and Baldwin.<sup>2,3</sup> Large cells with a free water level provide a means to obtain saturation profiles in the plugs that permit the simultaneous determination of both the positive and negative portions of the imbibition  $P_c$  curve in the plugs. Once the plugs were centrifuged for 2 weeks at 35° C, they were chilled while centrifuging to solidify the octadecane, removed and then imaged in the cells by both MRI and x-ray. The purpose of the imaging was to determine the free water level and obtain an indication of the  $P_c$  profile that can be seen above the free water. The free water level can easily be determined from the MRI images (Figure 3) or x-ray image profiles (Figure 5). These steps can be repeated if needed until the profiles indicate that fluids no longer move in the plugs. Once final images were obtained in the cells, the plugs were removed and imaged in the configuration previously measured for  $I_o$ . From these final images, once corrected for the slight variations seen by the reference plug, the local saturation state as a function of pixel height in the plugs was calculated from equations 1 and 2 above. Correlating the local saturation with the local pressure field induced by the centrifuge and the free water level for  $P_c = 0$  as measured from the images in the cells, the positive and negative portions of the imbibition  $P_c$  curves were obtained (Figures 6

through 9). These Pc curves are slightly truncated at the tops and bottoms of the image to avoid the same edge effects described above.

### **OBSERVATIONS/DISCUSSION/FOLLOW-UP**

The Pc curves that are obtained by the DMS method are a co-current imbibition process. With a sleeved plug, oil always enters or exits the end of the plug nearest the centrifuge axis and water always enters or exits the other end of the plug. For valid Pc curves, the wettability alteration of these plugs was assumed to be uniform. Wettability, if calculated by using the water saturation at the free water level where capillary pressure is zero, may not necessarily match the conventional Amott Index in which the numerator is determined by saturation from counter-current imbibition. Other authors have noted the difference in spontaneous imbibition oil recovery between co-current and counter-current displacement in various rock types.<sup>25,26,27</sup> The Pc curves obtained in this study indicate that Plug 10-1 (Figure 8) is highly water-wet and the other 3 plugs have altered wettabilities (Figures 6, 7, 9), but still appear strongly water-wet.

Follow-up measurements were conducted to evaluate the assumption of uniform wettability alteration of these plugs. Tests by spontaneous counter-current imbibition indicated considerable differences in the rate and volume of oil production between the plugs (Figure 10). This was not the imbibition behavior that should be expected from the measured Pc curves, except for plug 10-1. The rapid spontaneous imbibition for plug 10-1 was consistent with the measured Pc curve. Saturation profiles obtained at the termination of imbibition (Figure 11) resolved the reason for the discrepancies. For plugs 8-2 and 10-2, where the counter-current spontaneous imbibition rate and volume were less than that for plug 10-1, the corresponding post-imbibition saturation profiles showed little to no water saturation near both ends of these plugs (Figure 11 shows a comparison at the upper end of the plugs). This confirmed that the axial wettability of these plugs was non-uniform and had affected the spontaneous imbibition results. This can also be inferred from the long induction times prior to imbibition followed by a relatively short imbibition time. The spontaneous imbibition test for plug 8-1 was not completed, so no firm conclusions were drawn from that data. Since the linear x-ray images include the entire thickness of plug, radial wettability variations could not be obtained from the measured data for plugs 8-2 and 10-2. But with the average saturation from the post-imbibition saturation profile (52% and 50% for plugs 8-2 and 10-2, respectively) being greater than that obtained from the imbibition test data (Figure 10), it can be reasonably expected that a radial variation in wettability also existed. Consequently, the Pc curves obtained on the altered wettability plugs described herein are compromised. This would also be true for any other Pc methodology, but the wettability artifact would be unknown. However, the DMS methodology provides a means to obtain Pc curves using linear x-ray imaging and shows how to evaluate some of the assumptions built into such Pc curves.

### **CONCLUSIONS**

- 1) Lambert's corollary provides a straightforward method for calculating saturations in rock samples.
- 2) Linear x-ray imaging using Lambert's corollary can provide an accurate measure of Pc provided steps are taken to minimize artifacts.
- 3) An evaluation of assumptions, such as uniform wettability within plugs should be a part of the Pc curve measurement process.

## ACKNOWLEDGMENT

The authors are grateful to Phillips Petroleum Company for permission to publish and present this paper. Thanks are given to K. Farmer for his assistance in the laboratory.

## NOMENCLATURE

cc	Cubic centimeter	o	Subscript for oil
C	Celsius	Pc	Capillary pressure
DMS	Direct measurement of saturation	psi	Pounds per square inch
I	Emergent x-ray intensity	Sw	Water saturation
I <sub>0</sub>	Baseline I	t	Thickness
KI	Potassium iodide	w	Subscript for water
md	Millidarcy	%	Percent
MRI	Magnetic resonance imaging	μ	Absorption coefficient
mm	Millimeter	Φ	Porosity

## REFERENCES

1. Baldwin, B. A. and Spinler, E. A., "A Direct Method for Simultaneously Determining Positive and Negative Capillary Pressure Curves in Reservoir Rock," *Journal of Petroleum Science and Engineering*, (1998) **20**, 161-165.
2. Spinler, E. A. and Baldwin, B. A., "A Direct Method for Determining Complete Positive and Negative Capillary Pressure Curves for Reservoir Rock using the Centrifuge," *4<sup>th</sup> International Reservoir Characterization Technical Conference proceedings*, (1997)
3. Spinler, E. A. and Baldwin, B. A., "Capillary Pressure Scanning Curves by Direct Measurement of Saturation," *International Symposium of the Society of Core Analysts proceedings*, (1997) SCA paper 9705.
4. Sarwaruddin, M., Torsaeter, O., Skauge, A., "Comparing Different Methods for Capillary Pressure Measurements," *International Symposium of the Society of Core Analysts proceedings*, (2000) SCA paper 2051.
5. Wardlaw, N. C. and Taylor, R. P., "Mercury Capillary Pressure Curves and the Interpretation of Pore Structure and Capillary Behavior in Reservoir Rocks," *Bulletin of Canadian Petroleum Geology*, (1976) vol. 24, no. 2, pp. 225-262.
6. Purcell, W. R., "Capillary Pressures - their Measurement using Mercury and the Calculation of Permeability therefrom," *Petroleum Transactions, AIME* (Febr. 1949) pp. 39-48.
7. McCullough, J.J., Albaugh, F. W. and Jones, P. H., "Determination of the Interstitial-Water Content of Oil and Gas Sand by Laboratory Tests of Core Samples," *API Drilling and Production Practice*, (1944) pp. 180-188.
8. Thornton, O. F. and Marshall, D. L., "Estimating Interstitial Water by the Capillary Pressure Method," *Trans. AIME*, (1947) pp. 69-80
9. Bruce, W. A. and Welge, H. J., "Restored-State Method for Determination of Oil-in-Place and Connate Water," *Oil and Gas Journal*, (1947) vol. 46, p. 223
10. Rose, W. and Bruce, W. A., "Evaluation of Capillary Character in Petroleum Reservoir Rock," *Trans. AIME* (1949) vol. 186, pp. 127-142
11. Longeron, D., Hammervold, W. L., and Skjaeveland, S. M., "Water-Oil Capillary Pressure and Wettability Measurements Using Micropore Membrane Technique" *International Meeting on Petroleum engineering in Beijing, PR China proceedings*, (1995) SPE30006

12. Hammervold, W. L., Knutsen, O., Iversen, J. E., and Skjaeveland, S. M., "Capillary Pressure Scanning Curves by the Micropore Membrane Technique," *The 4<sup>th</sup> International Symposium on Evaluation of Reservoir Wettability and its Effect on Oil Recovery proceedings*, (1996)
13. Torsaeter, O., Determination of Positive Imbibition Capillary Pressure Curves by Centrifuging," *The 3rd International Symposium on Evaluation of Reservoir Wettability and its Effect on Oil Recovery proceedings* (1994)
14. Bolas, T. and Torsaeter, O., "Theoretical and Experimental Study of the Positive Imbibition Capillary Pressure Curves Obtained from Centrifuge Data," *1995 International Symposium of the Society of Core Analysts proceedings* (1995)
15. Fluery, M. Ringot, G., and Poulain R., "Positive imbibition capillary pressure curves using the centrifuge technique," *International Symposium of the Society of Core Analysts proceedings*, (1999) SCA paper 9913
16. Firoozabadi, A., Soroosh, H., and Hasanpour, G., "Drainage Performance and Capillary Pressure Curves With a New Centrifuge," *Journal of Petroleum Tech.*, (1988) pp. 913-919
17. Ruth, D. and Chen, Z., "Measurement and Interpretation of Centrifuge Capillary Pressure Curves - The SCA survey Data," *The Log Analyst*, (Sept.-Oct 1995) pp. 21-33
18. Bech, N, Olsen, D., Nielsen, C. M., "Determination of Oil/Water Saturation Functions of Chalk Core Plug from Two-Phase Flow Experiments," *SPE reservoir Eval. & Eng.* (2000) **3** pp. 50-59
19. Spinler, E. A., Baldwin, B. A., Graue, A., "Simultaneous Measurement of Multiple Capillary Pressure Curves from Wettability and Rock Property Variations within Single Rock Plugs," *International Symposium of the Society of Core Analysts proceedings*, (1999) SCA paper 9957
20. Tang, G., and Firoozabadi, A., "Effect of Viscous Forces and Initial Water Saturation on Water Injection in Water-Wet and Mixed-Wet Fractured Porous Media," *SPE/DOE Improved Oil Recovery Symposium proceedings*, (2000) SPE59291
21. Maloney, D., Wegener, D., and Zornes, D., "New X-ray Scanning System for Special Core Analysis in Support of Reservoir Characterization," *International Symposium of the Society of Core Analysts proceedings*, (1999) paper SCA9940
22. Bertin, E. *Principles and Practice of X-ray Spectrographic Analysis*. Plenum Press. New York, (1970)
23. Maloney, D., Wegener, D., and Zornes, D., "Significance of Absorption Coefficients When Determining In Situ Core Saturations by Linear X-ray Scans," *International Symposium of the Society of Core Analysts proceedings*, (2000) paper SCA2013
24. Forbes, P. L., Chen, Z. A., and Ruth, D. W., "Quantitative Analysis of Radial Effects on Centrifuge Capillary Pressure Curves," *SPE Annual Technical Conference and Exhibition proceedings*, (1994) SPE28182
25. Bourbiaux, B. and Kalaydjian, F. J., "Experimental Study of Co-Current and Counter-Current flows in Natural Porous Media" *SPE* (August, 1990) pp. 361-368
26. Terez, I. E., and Firoozabadi, A., "Water Injection in Water-wet Fractured Porous Media: Experiments and a New Model Using Modified Buckley-Leverett Theory," *SPE/DOE Improved Oil Recovery Symposium proceedings*, (1996) SPE39605
27. Bogno, T., Aspenes, E., Graue, A., Spinler E. A., and Tobola, D., "Comparison of Capillary Pressure Measurements at Various Wettabilities using the Direct Measurement of Saturation

Method and Conventional Centrifuge Techniques," *International Symposium of the Society of Core Analysts proceedings*, (2001)

**Table 1**  
**Core Plug Properties**

Sample No.	Grain Vol (cc)	Bulk Vol (cc)	Pore Vol (cc)	Porosity (fraction)	Grain Density (grams/cc)	Permeability (md)
8-1	13.85	20.94	7.10	33.89	2.73	3.05
8-2	9.18	14.42	5.24	36.36	2.70	4.17
10-1	14.00	21.19	7.20	33.95	2.73	3.92
10-2	13.98	21.22	7.24	34.13	2.73	3.85

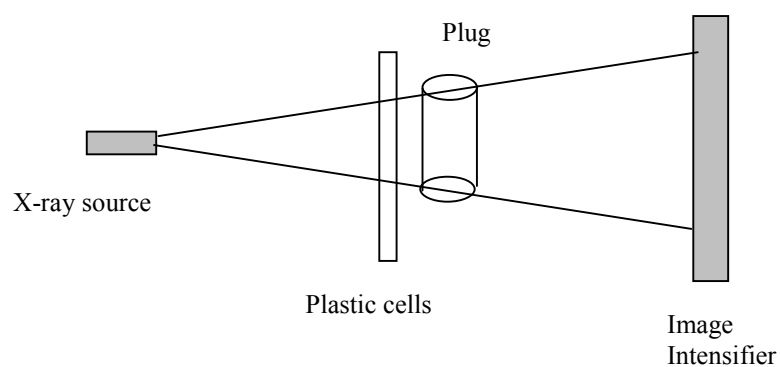


**Figure 1** - Layout of the x-ray apparatus

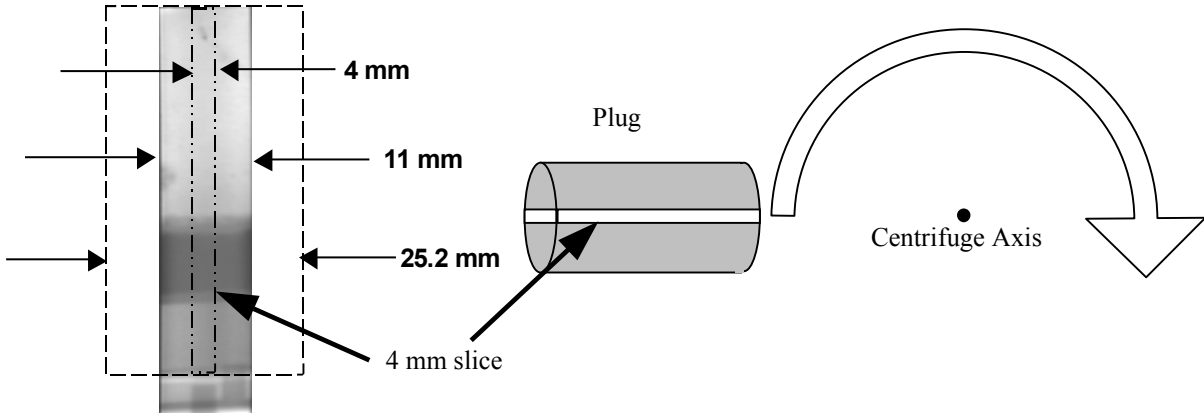


**Figure 2** - Placement of the analyzed 4mm slice of the x-ray image to reduce artifacts

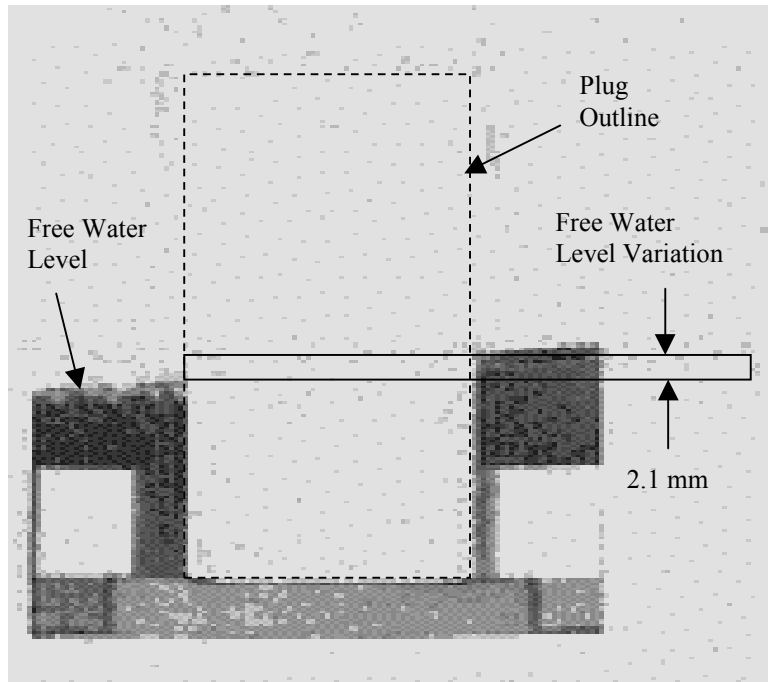


**Figure 3** A 2D image with a 4 mm depth by MRI perpendicular to the x-ray image showing the variation in the free-water level from gravity effects in the 4 mm x-ray image slice of Figure 2.

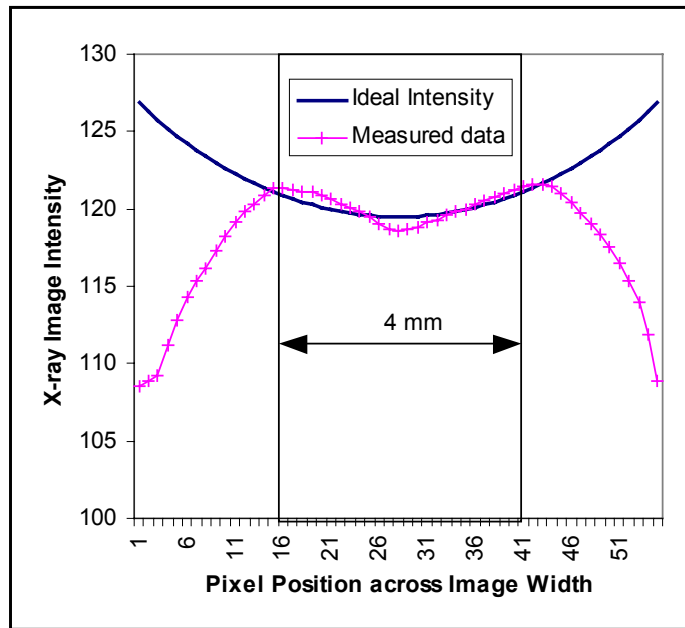


**Figure 4** One illustration of the edge effects near the sides of the image. The ideal curve shows the intensity increase that should occur from the plug's cylindrical shape.

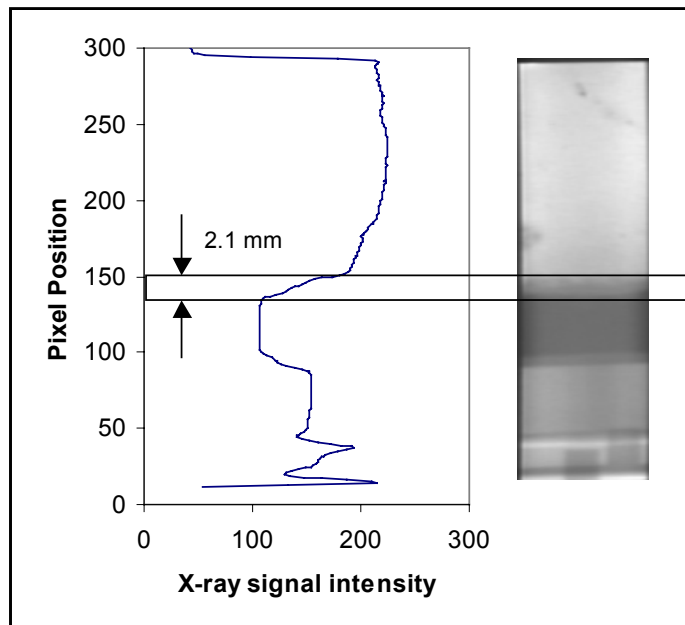


**Figure 5** A profile from an x-ray image of a plug in the cell also shows the position of the free water level.

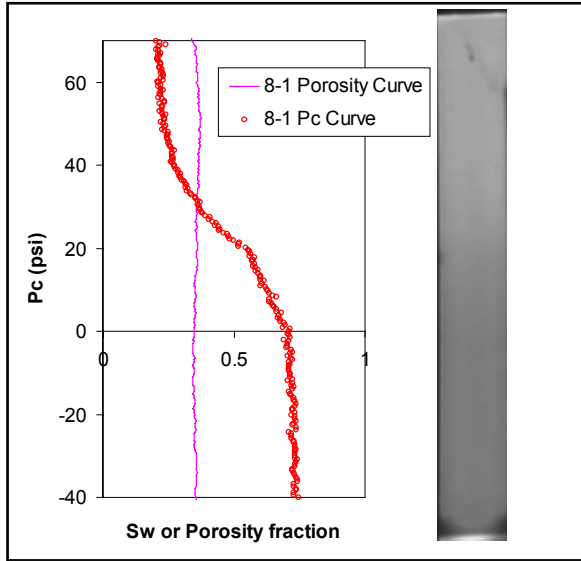


**Figure 6** The calculated Pc and porosity curves for altered-wettability plug 8-1 that appears water-wet. The x-ray image is the basis for the calculated Pc.

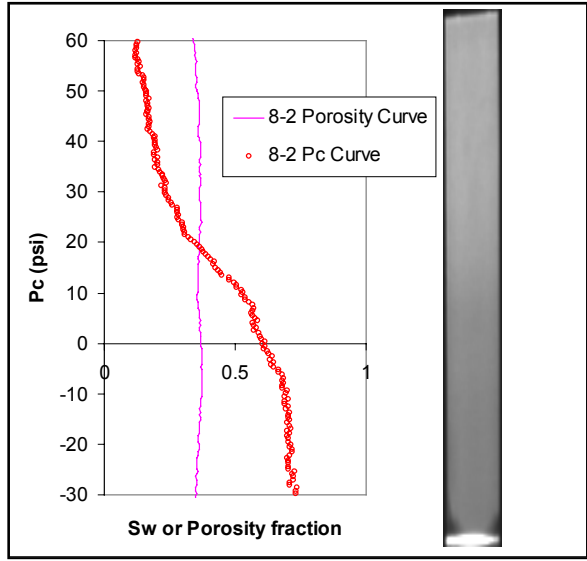


**Figure 7** The calculated Pc and porosity curves showing altered-wettability plug, 8-2. This plug is shorter than the other plugs resulting in a reduced pressure range.

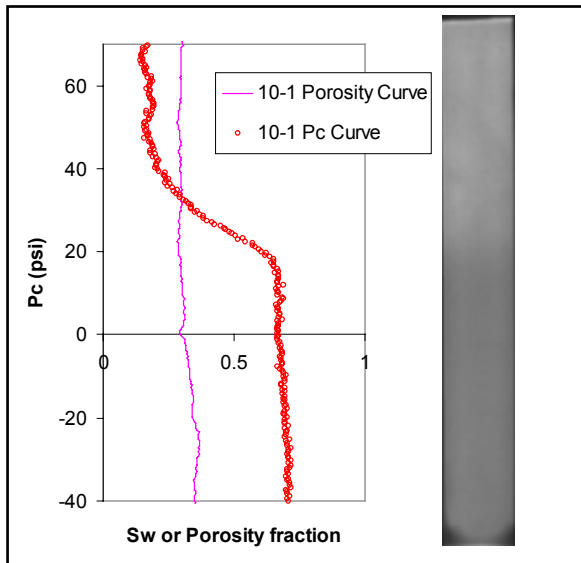


**Figure 8** The calculated porosity and Pc curves showing an unaltered-wettability plug, 10-1, which is highly water-wet.

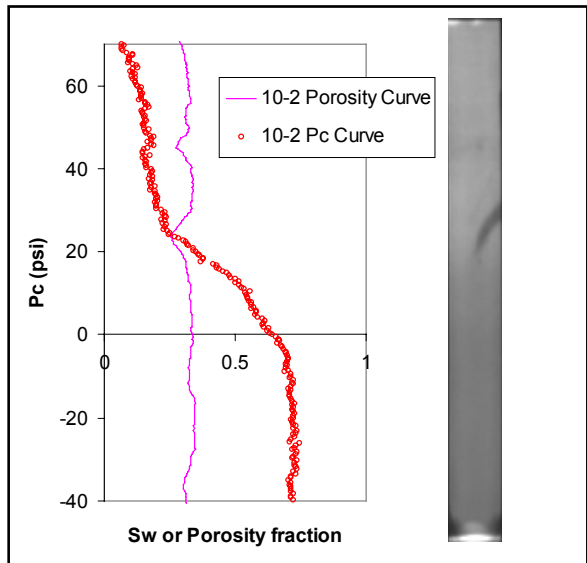


**Figure 9** The calculated Pc and porosity curves showing an altered-wettability plug, 10-2.

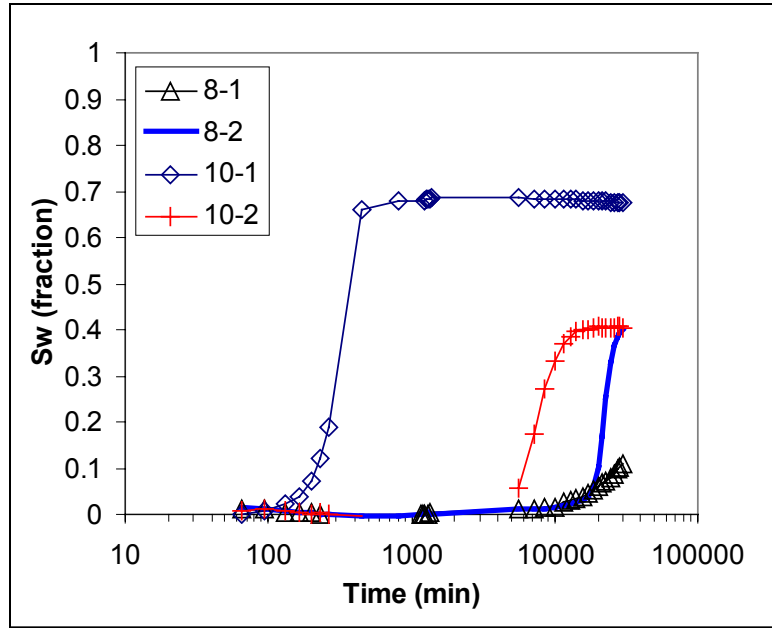


**Figure 10** Spontaneous counter-current imbibition production profiles.

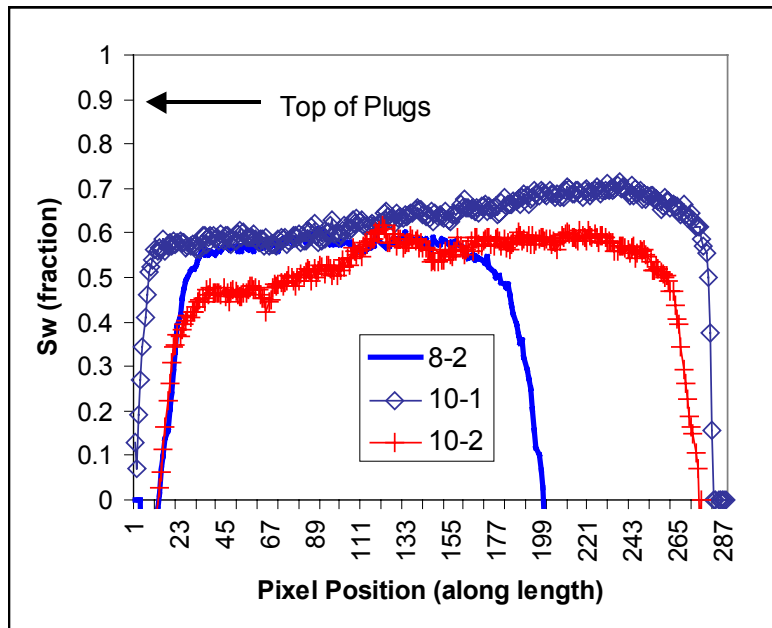


**Figure 11** Sw profiles from 3 of the plugs following the imbibition of Figure 10. The plugs are different lengths, but are aligned at the plug top to show differences in the profiles.